Unclassified

SECURITY CLASSIFICATION OF THIS PAGE (When Data Entered)

REPORT DOCUMENTATION PAGE	READ INSTRUCTIONS BEFORE COMPLETING FORM
1. REPORT NUMBER: AFGL-TR-80-0120	2. GOVT ACCESSION NO.: AD-A083 550
3. RECIPIENT'S CATALOG NUMBER	
4. TITLE (and Subtitle): A DISCUSSION OF ARCTIC IONOGRAMS.	5. TYPE OF REPORT & PERIOD COVERED: Scientific. Interim rpt.
	6. PERFORMING ORG. REPORT NUMBER
7. AUTHOR(s): R. A. Wagner, C. P. Pike	8. CONTRACT OR GRANT NUMBER(s)
9. PERFORMING ORGANIZATION NAME AND ADDRESS: Air Force Geophysics Laboratory (PHG), Hanscom AFB, Massachusetts 01731	10. PROGRAM ELEMENT, PROJECT, TASK AREA & WORK UNIT NUMBERS: 62101F, 56311401
11. CONTROLLING OFFICE NAME AND ADDRESS: Air Force Geophysics Laboratory (PHG), Hanscom AFB, Massachusetts 01731	12. REPORT DATE: 14 April 1980
	13. NUMBER OF PAGES: 22
14. MONITORING AGENCY NAME & ADDRESS (if different from Controlling Office)	15. SECURITY CLASS. (of this report): Unclassified
	15a. DECLASSIFICATION DOWNGRADING SCHEDULE

16. DISTRIBUTION STATEMENT (of this Report)

Approved for public release; distribution unlimited.

DTIC ELECTE APR 28 1980 S D A

17. DISTRIBUTION STATEMENT (of the abstract entered in Block 20, if different from Report)

18. SUPPLEMENTARY NOTES

Paper presented at AGARD Technical Meeting in Lindau/Harz, Germany in September 1971

19. KEY WORDS (Continue on reverse side if necessary and identify by block number)

Ionosphere
Airborne research
Aurora

20. ABSTRACT (Continue on reverse side if necessary and identify by block number)

Examples of arctic ionogram sequences, recorded on the AFCRL Flying Ionospheric Laboratory, are presented. The purpose of this paper is to show that: a) ionogram sequences, recorded on arctic flights, facilitate the interpretation of oblique incidence echoes from E- and F-layer heights, b) parameters of the arctic ionosphere can be mapped by using the "auroral oval" as an ordering system, c) vertical and oblique incidence echoes, appearing on ground station ionograms, can be interpreted in terms of the station's position to relative to the auroral oval.

DD FORM 1 JAN 73 1473 EDITION OF 1 NOV 65 IS OBSOLETE

Unclassified

SECURITY CLASSIFICATION OF THIS PAGE (When Data Entered)

409578

AD A083550

The analysis of a three hour flight with 6 latitudinal scans underneath an auroral band shows the close relationship between auroral type sporadic E echoes (E_{sa}) and discrete aurora. The investigation of 49 latitudinal scans through the auroral oval during times of low magnetic activity revealed the existence of a particle produced E layer which is oval aligned, is 2° to 6° wide in corrected geomagnetic latitude and occurs at all corrected geomagnetic times. This layer produces the night E echoes.

A new ionogram analysis procedure, which uses oblique incidence F-layer echoes, is demonstrated, and the feasibility of monitoring the latitude of the southern edge of the polar F-layer irregularity zone by using this new analysis procedure is demonstrated.

(Paper presented at AGARD Technical Meeting in Lindau/Harz, Germany in September 1971)

A Discussion of Arctic Ionograms

R.A. Wagner and C.P. Pike
USAF Cambridge Research Laboratories
Bedford, Mass., 01730, USA

SUMMARY

Examples of arctic ionogram sequences, recorded on the AFCRL Flying Ionospheric Laboratory, are presented. The purpose of this paper is to show that: a) ionogram sequences, recorded on arctic flights, facilitate the interpretation of oblique incidence echoes from E- and F-layer heights, b) parameters of the arctic ionosphere can be mapped by using the "auroral oval" as an ordering system, c) vertical and oblique incidence echoes, appearing on ground station ionograms, can be interpreted in terms of the station's position relative to the auroral oval.

The analysis of a three hour flight with 6 latitudinal scans underneath an auroral band shows the close relationship between auroral type sporadic E echoes (E_{sa}) and discrete aurora. The investigation of 49 latitudinal scans through the auroral oval during times of low magnetic activity revealed the existence of a particle produced E layer which is oval aligned, is 2° to 6° wide in corrected geomagnetic latitude and occurs at all corrected geomagnetic times. This layer produces the night E echoes.

A new ionogram analysis procedure, which uses oblique incidence F-layer echoes, is demonstrated, and the feasibility of monitoring the latitude of the southern edge of the polar F-layer irregularity zone by using this new analysis procedure is demonstrated.

1. INTRODUCTION

Vertical incidence ionograms, recorded in high latitude regions, are often highly complex. Spread echoes and a variety of oblique echoes, which originate in E- and F-layer heights of the ionosphere, complicate ionograms. In E-layer heights different types of echoes are often simultaneously observed, and their appearance may change rapidly. These complications are the well-known cause of the difficulties which are encountered in scaling and interpreting of arctic ionograms.

It is often difficult to interpret echoes on complex ionograms when only individual sweeps, recorded at long time intervals, are considered. Ionogram analysis and interpretation can be aided by using ionogram sequences. This technique was used for instance, by Hanson et al(1) to show movements of the night E-layer, and is presently being used in recording vertical incidence swept frequency ionograms on the AFCRL Flying Ionospheric Laboratory. An ionospheric sounder, carried on a high-speed aircraft, is a valuable tool for investigating the arctic ionosphere.

For planning arctic flights the "auroral oval" (Feldstein and Starkov, (2)) has been used as a frame of reference, since it has proved to be an ordering system for many arctic geophysical phenomena. The auroral oval, defined as the region of maximum occurrence of visible aurora at a given instant, is an oval shaped belt surrounding the geomagnetic pole. The oval's position is fixed with respect to the sun and the earth rotates underneath it. A high-speed aircraft, flying at high latitudes against the earth's rotation, can stay at constant CG local time for many hours while, at the same time, making latitudinal scans. By flying in the direction of the earth's rotation the aircraft's movement relative to the oval can be accelerated, and the entire oval can be investigated in one 10 hour flight. The corrected geomagnetic (CG) coordinate system (Hultquist, (3), (4), Hakura, (5)) is used throughout this paper.

Examples are discussed in this paper which demonstrate the usefulness of ionogram sequences, recorded on flights and on the ground, in interpretation of oblique incidence echoes from E- and F-layer heights. Analysis of ionogram sequences, accumulated in cross-section flights through the auroral oval at all CG local times, has permitted the mapping of the occurrence of auroral E and auroral E_s relative to the location of the auroral oval. A special analysis procedure, which uses oblique incidence F-layer echoes for monitoring the latitude of the southern edge of the polar F-layer irregularity zone, is presented.

2. E REGION

Many statistical investigations and single case studies have been made of the relationship between ionospheric E-region echoes and the visual aurora.

Results, obtained from simultaneous ionogram recordings and observations of aurora, show that good correlation exists between: a) sporadic E (E_s) range and elevation of aurora (Knecht (6), Buchau et al. (7), Whalen et al. (8)), b) auroral brightness and the top frequency of E_s echoes (Knecht (6), Hunsucker and Owren (9)), c) auroral brightness and the inverse of the virtual height of E_s echoes for the case of overhead aurora (Harang (10), Knecht (6)). The results of the work of many researchers are reconsidered in relation to the auroral oval, in a study of the distribution of occurrence of E_s in high latitudes, by Pittenger and Gassmann (11). E_s echoes with top frequencies >5 MHz were found to occur in an oval pattern and to have a pronounced maximum in the oval's night sector, indicating a close relationship to the location of maximum occurrence of visual aurora.

Simultaneous occurrence at a station of night E (or "auroral E", a term proposed by Penndorf (12) for this particle produced layer) and aurora has been reported by King (13) and Bullen (14). On the other hand Hanson et al. (1) found no hour-to-hour correlation of night E with aurora. Night E has also been observed equatorward of visual aurora (King (15)). With increasing magnetic activity auroral E (night E) is observed at lower latitudes than in quiet conditions, which suggests a relationship between auroral E and the auroral oval. Whalen et al. (8) found close relation between non-discrete, continuous aurora and auroral E (night E) on cross-section flights through the noon sector of the auroral oval.

Observations of the relationship between E_{sa} echoes and aurora and between night E and the location of the auroral oval, reported here, were made during cross-section flights through the auroral oval.

2.1. RELATIONSHIP BETWEEN AURORAL E_s AND VISUAL AURORA

A section of a flight is discussed where the aircraft crossed several times underneath a stable auroral band. Vertical incidence ionograms and all-sky photographs used for this analysis were simultaneously recorded at one minute intervals on 14 December 1968 during a flight from Labrador to Alaska. The flight track was planned so that the midnight sector of the auroral oval could be monitored for more than 9 hours while 18 latitudinal cross-sections, extending over 3° to 3-1/2° CG latitude, were made within the auroral belt. Recording of ionograms and all-sky photographs started on scan 4 and continued through the end of the flight. The flight track is shown in Figure 1 in geographic coordinates on the left side and in CG latitude and CG local time on the right side.

Quiet magnetic conditions prevailed during the flight, $K_p = 0+, 1, 1$. In the first part of the flight no discrete aurora was observed, and only occasional brightening of the sky and very faint unstructured forms in the north were observed. No E_s was recorded during this time; however, a band of auroral E was observed which will be discussed later. At 6 UT (at the start of latitudinal scan 7) an oval-aligned arc developed which extended from the west to the east horizon. During the following 6 hours this aurora was seen constantly while the aircraft moved to the west, crossing underneath the aurora from south to north respectively north to south 12 times. In the last three hours of the flight (9 to 12 UT) the aurora was at times very active often filling the entire field of view of the all-sky camera (1000 km diameter); quiet conditions returned in between. During the 6 hours when discrete aurora was observed auroral E_s was recorded continuously; auroral type E_s, as described in the IGY Manual (16), page 94—95. Figure 2, lower part, shows an E_{sa} echo recorded during this flight. When the aircraft approached an arc or band, passed underneath it, and then moved away from it, the virtual height of the E_{sa} echo regularly decreased from high ranges, levelled off at a minimum value and increased again. When overhead aurora was observed over the entire width of the latitudinal scans, the time history of any of the individual bands or other forms could not be followed, the $h'E_{sa}$ stayed at minimum values, no oblique traces were seen. As soon as a band or arc could again be defined and it's zenith angle determined, the time variation of $h'E_{sa}$ and of the slant ranges to the aurora coincided again.

In the upper part of Figure 3, the virtual height of E_{sa} (open circles) and the slant ranges to the visible aurora (full circles connected by dotted line) are plotted versus UT. They were recorded during the 3 hours when a stable auroral arc or band was crossed 6 times. Encircled numbers indicate the scan number in the sequence of latitudinal crossings. The slant ranges to the aurora were determined from the all-sky photographs assuming that the lower edge of the aurora was 120 km above ground. The slant ranges to the aurora and $h'E$ coincide very well. Approach to and movement away from the aurora can be followed in passes 9 through . since the location of the bands (extending east-west) was in the center latitude of the scans. In scan 7 the aircraft turned before reaching the northern edge of the aurora, and on the return scan the southern edge had moved to the north. The fact that the virtual height of the E_{sa} and the slant range to the aurora change simultaneously during the 6 crossings underneath the auroral band indicates that the region of ionization, causing the E_{sa} echoes, must be limited in latitudinal extent to the vicinity of the discrete aurora.

The auroral brightness increased during the period investigated. During passes 7 and 8 the aurora was very faint, $h'E_{sa}$ was 130-135 km when the aurora was overhead. Increased auroral brightness was observed in passes 9 and 10, the recorded minimum virtual height of E_{sa} was 120 km when the aurora was overhead. Finally, (passes 11 and 12) $h'E_{sa}$ had decreased to 105 km, and the brightness of the overhead aurora had again increased. From 0610 to 0730 UT (i.e. pass 7 through most of pass 9) simultaneous photometer measurements of the 5577Å emission were made (Whalen, private communication). When visible aurora was overhead during this time, the correlation between the spectral line intensity and the inverse virtual height of E_{sa} is good, even for short-time fluctuations.

Assuming that the height above ground of the lower edge of the auroral form, is identical with the virtual height of the E_{sa} when the aurora is in the aircraft zenith, the slant ranges were replotted for passes 7, 8, 11 and 12; The improved fit of the resulting slant ranges to the aurora and $h'E_{sa}$ curves is shown in the lower part of Figure 3. (Arrows below the time scale in pass 12 indicate the times for which ionograms and all-sky photographs are shown later, in Figure 5).

The correlation between auroral brightness and top frequency (fE_{sa}) of the E_{sa} echoes, found by other investigators, is confirmed by the measurements of this flight: faint aurora from (6-7 UT) is accompanied by fE_{sa} only occasionally over 4 MHz; increased auroral brightness (from 7-8 UT) by $fE_{sa} \approx 5$ MHz; rather bright aurora (from 8-9 UT), by fE_{sa} between 8 and 9 MHz. Therefore, it follows that the $h'E_{sa}$ is inversely related to fE_{sa}. In Figure 4 the virtual height of E_{sa}, recorded in passes 7 through 12 when aurora was observed in the zenith, are plotted versus the top frequency of the E_{sa} echo.

Figure 5 gives examples of ionograms and all-sky photographs recorded on pass 12. Simultaneously recorded ionograms and all-sky frames are labelled a. through d. and show that the range of the E_{sa} echo decreases when the auroral band is approached. Arrows below the time scale (pass 12) of Figure 3, lower part, indicate the times when the frames were recorded.

2.2 OCCURRENCE OF AURORAL E (NIGHT E) IN RELATION TO THE AURORAL OVAL

The close association between E_{sa} echoes and discrete aurora has been demonstrated. A few examples follow of the occurrence of auroral E (night E) echoes in relation to the auroral oval. The auroral E (night E) echoes were identified according to the description on page 106 of the IGY Manual (16). This definition, originally given by Hanson et al. (1), was found to be clear and comprehensive. Figure 2, upper part, shows two examples of auroral E (night E) echoes, recorded during arctic flights. A band of auroral E (night E) was regularly found in the three flights of December 1968 with a total of 16 cross-sections of the auroral oval at CG noon in darkness, reported by Whalen et al. (8). Characteristics of this particle

produced continuous E layer that are of interest here, are as follows: In the noon sector it extends about 5° southward from the instantaneous location of the discrete aurora; at the northern edge, at the location of overhead aurora, the typical E-echoes transform to E_{ss} at the same virtual height; from north to south the critical frequency of the auroral E layer increases, while the virtual height decreases.

Subsequent investigations of ionogram sequences from cross-section flights through other sectors of the auroral oval confirmed the existence of an oval aligned E- layer of particle origin.

AURORAL E OBSERVED IN THE NIGHT SECTOR OF THE AURORAL OVAL

In Figure 6 the tracks of cross-section flights through the night sector of the auroral oval are shown. The flights were made during the time from February 1968 through February 1971, and they were selected for this survey because of quiet magnetic conditions during the flights. Kp indices were 0 to 2 during most of the time; exceptions are $K_p = 3$ for part of flights d and e, and $K_p = 4-$ at the start of flight b. A total of 33 latitudinal scans through, or within the night sector of the oval were made along the flight tracks; flights d, e, and f are "oval stationary" flights with several scans in the same CG time sector; 2 flights were made along flight route c. The heavy dotted lines indicate the flight tracks where auroral E (night E) with critical frequencies ≥ 2 MHz was observed; 2 MHz being the low frequency limit of the airborne sounder. Auroral E occurs in a continuous band that extends over several degrees of latitude. A black bar across the flight track indicates the location of the maximum critical frequency recorded on that scan. In the oval stationary flight d auroral E was present continuously in all 6 scans; in 3 or 4 scans for flight e; and in 5 out of 15 scans for flight f. The f_oE maximum was found at identical latitudes in every scan of a particular oval stationary flight. This is true also for the second maximum at 69° CG latitude in flight e. In the last of the 4 scans of flight e nondeviative absorption had increased, auroral E with $f_oE < f\min$ may have been present.

Flight f is the flight of 14 December 1968 where, as mentioned before, no auroral bands or arcs were observed in the first part of the flight, only some barely visible forms and areas of brightness were noticed. Auroral E was observed continuously until E_{ss} appeared simultaneously with the auroral arc that had formed. (Occasionally oblique E echoes could be seen in the presence of E_{ss}.) This observation confirms the relation of auroral E and a non-discrete form of aurora, found in the noon sector of the auroral oval (Whalen et al. (8)). For all other flights the location of the band of night E relative to the position of discrete aurora is not investigated here.

In the latitudinal distribution of f_oE a second maximum, as seen in flight e, is sometimes observed during more disturbed conditions. Concluding from the results of Whalen et al. (8), electron precipitation with a spectrum, hardening equatorward, is likely responsible for the auroral E-layer. Proton precipitation was found to be the cause for a second maximum in the north, recorded in a previous flight and not included here. Conditions in flight e are still under investigation. No second maximum of f_oE was observed in the other flights shown in Figure 6. In flights b and d, and perhaps in some scans of f, the auroral E (night E) region may have extended farther to the north of the flight tracks, and a second maximum may, therefore, have escaped observation. However, no increase in the E critical frequency was indicated near the northern end of the scans. Figure 6 summarizes the observations of cross-section flights through the night sector of the auroral oval in quiet magnetic conditions: a) Auroral E occurs in bands several degrees wide in latitudinal extent; and b) the pattern of f_oE increase with decreasing latitude that was established for the noon sector in darkness, is found to exist in the night sector also.

ENHANCED f_oE IN THE DAY SECTOR OF THE AURORAL OVAL, IN SUNLIGHT

Particle produced ionization in E-layer height has also been observed in the sector 08 through 21 CG time for times of low magnetic activity under sunlit conditions. In daylight the normal E-layer is produced by photoionization; where particle precipitation causes additional ionization, an enhanced critical frequency of the E layer is measured, with an f_oE that is higher than that corresponding to the zenith angle of the sun at that given time and location. Figure 7 shows (plotted in CG latitude and CG time) the routes of 9 flights performed in the summer of 1970 and 1971 which yielded a total of 16 cross-sections through the auroral oval. All flights were made in daylight and during magnetic conditions characterized by K_p 0 to 3- (except for one crossing with K_p 4-). Heavy black lines along the flight tracks indicate the latitudes where enhanced f_oE was recorded. Dotted lines indicate those areas where the enhancement was very little. In every crossing of the oval a single belt of enhanced f_oE was observed, the latitudinal extent of which varied from 2° to 6°. Considerable variation in the location of the enhanced f_oE region is observed mainly in the 6 crossings in the 10 to 14 CG time sector. The center latitude of the region is located between 67° and 73° CG latitude compared with 71° and 78° for 16 crossings through the noon sector in darkness on the 3 flights of December 1968. In the evening, 18 through 21 CG time, the center latitude of the region of enhanced E ionization is found at 70° to 71° CG latitude in 5 out of 8 cases. This coincides with the results from cross-section flights during the same time interval, presented in Figure 6.

SPREAD E

Characteristic of the auroral E (night E) echo trace observed during dark hours is the spread near the critical frequency. Spread near the critical frequency of the E layer is also observed in ionograms recorded in the region of f_oE enhancement, in daylight. The spread E is observed so regularly with enhanced f_oE that Bullen (14) uses occurrence of spread E in daytime ionograms as one criterion to determine from ionograms the existence of particle produced ionization. In Figure 8 an example is given to illustrate the change in appearance of the E echo traces from normal to spread and back to normal. The ionograms were recorded during a flight in daylight across the oval belt. Within the latitude band where foE was enhanced, spread E was observed continuously. However, on the return (N to S) when the aircraft crossed the region of enhanced E again, the spread near the critical frequency of E was rather weak and not seen in every ionogram (one ionogram per minute being recorded).

AURORAL E OBSERVED CONTINUOUSLY AROUND THE AURORAL OVAL

The cross-section flights through the auroral oval belt at nearly all times accumulated statistical evidence for the validity of the E layer pattern which was first established for the noon sector in darkness. The question arises whether this pattern is also valid as an instantaneous picture around the auroral oval.

In the 10 hour circumoval flight of 5 January 1970 nearly the entire oval belt was investigated. In Figure 9 the thin continuous line is the flight track plotted in CG latitude and CG local time. The decrease of f_0E with increasing CG latitude was found in all sections of the flight where the flight track deviated from its primarily eastward course and crossed through several degrees of latitude toward the N or the S. This latitudinal dependence is particularly evident from 7 to 9 CG local time, 14 to 16 CG local time, and at the end of the flight near midnight. Using the f_0E values from analysis of the ionograms recorded during the flight, contour lines of f_0E were drawn, shown as heavy lines in Figure 9; the dotted lines connect extrapolated values. At 02 and 04 CG local time (in Figure 9) E echoes were seen obliquely; they originated from a layer S of the flight track, as could be determined by photometric measurements. The figure presents a quasi-instantaneous picture of the occurrence of auroral E (night E) as derived from data taken on this flight. The 5th of January 1970 was a day of low magnetic activity.

GROUND STATION DATA REVIEWED IN RELATION TO OVAL-ALIGNED E LAYER PATTERN

The E layer pattern for quiet days, derived from the aircraft data, can be tested by ground station data. As an example in Figure 10, in the center, a graph is shown from Hanson, et al. (1) of the time variation of the critical frequency of a night E echo observed during a 5 hour period at Fort Chimo on 26 January 1952, a magnetically quiet day. The ionograms, from which the critical frequencies are derived, are reproduced in their paper and show typical examples of night E (auroral E) echoes. The hour by hour positions of the station relative to the Q=1 auroral oval are marked by triangles, the first corresponding to 16 LT (local time at Fort Chimo). If on this day an approximately oval-aligned E region was present as indicated, the station would be south of the E region through about 1745 LT. Rotating further toward the auroral oval it would move under the 3.0 MHz f_0E contour at 18 LT. Due to the steep gradient versus latitude in f_0E at the southern edge of the E region, the narrow band of maximum f_0E is overhead before 19 LT. From 19 to 20 LT the station moves through the northern part of the night E region.

2.3. SUMMARY AND RESULTS

1) Analysis of ionogram sequences and simultaneous all-sky photographs from a flight making six latitudinal scans in the midnight sector of the auroral oval under quiet magnetic conditions shows that: a) The recorded auroral type Es echo (E_{sa}) is returned from a spatially limited area confined to the latitudinal extent of the visible aurora, b) Good correlation exists between the brightness of aurora in the zenith, the inverse of the virtual height of the E_{sa}, and the top frequency of the E_{sa}. Consequently, in case of overhead aurora, the top frequency increases with decreasing virtual height of the E_{sa}. The results of the analysis also appears to support the assumption that the E_{sa} echoes originate from a height identical with that of the lower edge of the aurora.

2) Ionogram sequences from cross-section flights through the oval belt during times of low magnetic activity show the existence of an oval-aligned region of auroral E (night E) which has a width of 2°-6° latitude. It extends equatorward from the location of the auroral oval in the day sector of the auroral oval and is located within the oval belt in the night sector. Of a total of 49 latitudinal scans through the oval belt, at times from 07 through noon to 04 Corrected Geomagnetic Time, 38 show the presence of auroral E. 16 of the 22 scans through the auroral oval's night sector exhibit the same latitudinal pattern found (by Whalen et al. (8)) in the noon sector in darkness; namely, decrease of virtual height of the E layer from north to south corresponding to precipitating particles with a hardening of the spectrum from northern to southern latitudes; and an increase of the E layer critical frequency from north to south. The analysis of day flights through the auroral oval resulted in the mapping of the regions where enhanced foE was recorded, i.e. where f_0E was higher than to be expected from photoionization. Although the latitudinal distribution of the amount of f_0E enhancement was not established here, the pattern is consistent with that derived from the measurements in darkness, as are the results of a 10 hour circumoval flight in which auroral E (night E) was continuously observed.

3. POLAR F-LAYER

The high-latitude F layer has been investigated by many workers, and several basic features are now known. Muldrew (18), using Alouette topside ionograms, first showed the existence of the main F-layer trough. Petrie (19) established that the occurrence of spread F on Alouette ionograms maximized in an oval-shaped region which encircled the geomagnetic pole. Akasofu (20) later identified Petrie's spread-F region as being coincident with the quiet time auroral oval, hence a "spread-F oval". Thomas and Andrews (21) showed that the distribution of topside F-layer electron density enhancements, scaled from Alouette ionograms, maximized in an elongated ring, the "plasma ring", which, similar to the spread-F oval, encircled the geomagnetic pole. Ionograms recorded on the Flying Ionospheric Laboratory during cross-section flights through the day sector of the auroral oval were compared with Alouette electron density data and showed that the topside polar F-layer plasma ring existed in the bottomside as an F-layer irregularity zone (22). On these flights the latitudinal extent of the F-layer irregularity zone was determined from ionogram movies recorded on the aircraft sounder. An example which illustrates how the aircraft's motion is used to interpret F-layer features on ionograms is shown in this next section.

3.1. AIRBORNE F-LAYER MEASUREMENTS

In the top half of Figure 11 the aircraft's flight route on August 22, 1970 is indicated by the dashed line drawn on a CG latitude and CG local time grid. The night sector of the auroral oval for Q=2 magnetic conditions is indicated by heavy solid lines. A sequence of aircraft ionograms is shown in the bottom-half of Figure 11. The letters next to the ionograms refer to the aircraft's positions, marked by the same

letters on the flight route map, when the ionograms were recorded. In ionogram A there is a vertical incidence F-layer echo at 280 km, the first and second F-layer multiple echoes, and an extra echo at about 425 km. In ionogram B the extra echo is at a range of about 490 km; while in ionogram C, recorded just before the aircraft turned, the extra echo is at a range of about 530 km. The change in range of the extra echo corresponds to about the distance that the aircraft flew away from the southern edge of the oval between the times ionograms A and C were recorded. The extra echo is then an oblique incidence echo which, most likely, is produced by a reflecting surface located north of the aircraft near the oval. Ionograms D and E show the oblique incidence echo moving down in slant range as the aircraft flies back towards the oval. In ionogram F the oblique incidence echo is now closer in slant range than the vertical incidence F-layer echo. Thus, the original vertical incidence F-layer echo is an oblique incidence echo, and a new F layer, the original oblique incidence echo, is moving down in range and will become a vertical incidence F-layer echo. The slant range to the extra echo is plotted versus universal time in Figure 12. The letters on the abscissa refer to the aircraft's positions which are noted in Figure 11 by corresponding letters. All of the ionograms, recorded at the rate of one per minute, contain a strong oblique incidence echo, therefore, the slant range to the oblique incidence echo could be plotted with an accuracy of ±10 km. One sees a uniform increase in slant range as the aircraft flies south, away from the oval. The inflection point of the curve corresponds to the time during which the aircraft turned, and the decrease in slant range is due to the aircraft flying north, towards the oval. This example demonstrates how F-layer echoes, which occur in a sequence of ionograms, can be uniquely identified and followed when the aircraft is flying relative to a stable reflector.

3.2. F-LAYER MEASUREMENT AT GOOSE BAY

From October 27-29, 1970 the Flying Ionospheric Laboratory was located on the ground at Goose Bay, Labrador. Goose Bay is located at geographic coordinates 54°N, 60°W or at CG coordinates 65.5°N, 22°W. The location of Goose Bay, indicated by triangles, and the Q=3 auroral oval have been plotted in Figure 13 on a CG latitude and time grid. From Figure 13 one can see that Goose Bay moves towards the oval during the afternoon and evening, that Goose Bay is underneath the oval near midnight, and that Goose Bay moves away from the oval in the morning. During this three day period at Goose Bay the aircraft sounder was operated continuously; the photometer and auroral all-sky camera were used at night for auroral measurements. Vertical and oblique incidence F-layer echoes, seen on the Goose Bay ionograms, are discussed here; schematic drawings, showing the main F-layer trough and the F-layer irregularity zone, are presented.

A sequence of Goose Bay ionograms, recorded on October 27, 1970, is shown in Figure 14. These ionograms were recorded during the late afternoon and evening from 1720 to 2110 local time, and F-layer sunset occurred at about 1830 local time. Analysis of these ionograms, recorded on 35 mm film, was facilitated by viewing a 16 mm movie of the ionograms a number of times and by following F-layer features frame by frame in the movie. Later, these features were identified and numbered on these single 35 mm frames. Ionogram A shows well defined ordinary and extraordinary wave components of an echo, labelled I, from an F layer produced by the sun and an extra echo, labelled III, at 725 ± 20 km between the first and second solar F-layer multiple echo. Ionogram B shows that echo III has moved down in range to 625 ± 20 km and has become better defined than before. The movie presentation of the ionograms, recorded between these two selected frames, shows echo III moving down in range. Ionogram C shows the solar F-layer echo, echo I, the first solar F-layer multiple echo, labelled I', echo III, and a new extra echo, labelled II, at 475 ± 10 km. Echoes, similar to those labelled II and III, have been identified by Stanley (23) and Bowman (24) as echoes which are produced by oblique incidence reflections from the poleward wall of the main F-layer trough. Echoes II and III are also similar to the oblique incidence echo that was reflected from the region of the oval in the airborne ionogram sequence in Figure 11. Thus, echoes II and III are probably oblique incidence echoes which are produced by reflecting surfaces located north of Goose Bay in the vicinity of the main F-layer trough and the F-layer irregularity zone. Ionogram D shows the solar F-layer echo, echo I, with no multiple echoes and the oblique incidence echo, echo II. The absence of a solar F-layer multiple echo would suggest that at this time a curvature in the structure of the plasma frequency contours is passing over Goose Bay and is causing ionospheric defocussing. Further suggestion for the presence of a curvature is the 30 km increase in virtual height of the solar F-layer echo which occurs between ionograms B and D. In ionogram E one sees echo I from the solar F layer, oblique incidence echo II, and what may be the reappearance of oblique incidence echo III. Bates (25) has pointed out that since aspect sensitivity of the reflecting surface is a problem encountered in the analysis of oblique incidence echoes, the appearance and disappearance of oblique incidence echoes can often be impossible to follow. Ionogram F contains a complex overlapping of echoes I, II, and III between 275 and 400 km which cannot be interpreted with certainty. However, a multiple reflection of echo II may now be seen; thus, echo II must be nearly overhead at this time.

A sequence of schematic drawings of F-layer structure, which could produce echoes I, II, and III, can provide some understanding of the ray path geometry involved in producing these echoes. The schematics, seen in Figure 15, were drawn by assuming that during the late afternoon and evening the main F-layer trough and the F-layer irregularity zone would move from the north towards Goose Bay. The schematics are composed of constant plasma frequency contours which extend north and south from Goose Bay. One schematic cross-section has been drawn for each ionogram in Figure 14. Virtual heights and plasma frequencies, taken from ionograms A through F, were used as the quantitative basis for the respective schematics. The earth's curvature was taken into account when the grid for the schematics was drawn. The ionosonde in the aircraft has a frequency threshold of 2 MHz. The trough, which has an f_0F2 equal to or less than 2 MHz (18) (23), was not seen directly on the ionograms, and its presence has been inferred by ionogram interpretation. Schematic A shows the plasma frequency contours which could produce the echoes in ionogram A. The solar F-layer echo, echo I in ionogram A, can be produced by ray path I in schematic A. Echo III can be produced by ray path III which has been constructed by assuming that a reflecting surface is located north of Goose Bay at about the 250 km level. Accordingly, the 725 km slant range to echo III in ionogram A corresponds to a northward horizontal distance of about 650 km as is shown in schematic A. The reflecting surface has been assumed to be the F-layer irregularity zone and has been represented in the schematics by a kink in the plasma frequency contours. In schematic B the irregularity zone is closer to Goose Bay than in schematic A, while in schematic C the distance between Goose Bay and the irregularity zone has not changed. These distances are consistent with the slant ranges to echo III which are seen in ionograms B and C. The appearance of echo II in ionogram C is interpreted as indicative of the onset of the trough. The formation of the trough would be expected

at this time because solar production, which fills in and smooths over the trough during daytime (26), has almost ceased by now. The shape of the trough has been drawn by using Bowman's (24) trough contours as a model with the exceptions that the troughs, which he saw during the IGY, were wider by a factor of 4 or 5 and deeper than the trough shown here. In ionogram D the absence of multiple echoes suggests that the trough is passing near Goose Bay at this time and is causing defocussing. For this reason, the trough is shown nearly overhead of Goose Bay in schematic D. Echo III is missing in ionogram D. One reason for this may be aspect sensitivity of the reflecting surface or, as indicated in the schematic, E_s or absorption may be blocking radio waves from reaching the irregularity zone. In schematic E ray path III is drawn because ionogram E may contain echo III. The trough has been drawn with about the same shape in schematic E as it had been drawn in schematic D. Because ionogram F contains a very complex overlapping of echoes, the interpretation given to these echoes in schematic F should be treated with caution. The appearance of a multiple echo of echo II, which up to now had been oblique and did not display a multiple echo, suggests that the trough has passed over Goose Bay and that Goose Bay is now located on the poleward side of the trough. Echoes I and III are barely discernable in ionogram F but, after examining other ionograms which were recorded at about the same time as this ionogram, the complex overlapping of these echoes has been interpreted as seen in schematic F. That is, it appears that echo I has moved out in range since the time that ionogram E was recorded; while echo III appears to have moved down in range since then.

3.3 MONITORING THE F-LAYER IRREGULARITY ZONE

In this section a new ionogram analysis procedure is presented, and examples are shown which demonstrate how this procedure can be used to monitor the CG latitude of the southern edge of the F-layer irregularity zone. A slant range plotter has been constructed so that the virtual heights of oblique incidence echoes, similar to those labelled III in Figure 14, could be utilized in ionogram analysis and not omitted as they generally are. This plotter (shown in Figure 16) permits the virtual height of an oblique incidence echo to be plotted versus the left ordinate; the CG latitude, which corresponds to an echo at this slant range, has been labelled on the right ordinate. Thus, the CG latitude of the F-layer irregularity zone can be monitored during the late afternoon and evening, when the irregularity zone is far to the north of Goose Bay, by plotting the virtual heights of Echo III onto the slant range plotter. A 250 km F-layer reflection height has been assumed for reflections which come from the F-layer irregularity zone. Some error in determining the latitude of the southern edge of the irregularity zone may be introduced by this assumption but it should not be greater than $\pm 0.5°$. The slant ranges to echo III in the October 27 ionograms have been plotted on the slant range plotter in Figure 16. The squares indicate that reflections from the irregularity zone were clearly seen at that particular time; while a series of squares, connected by a line, indicates that the irregularity zone echo was seen on each ionogram recorded during this period. The irregularity zone echo closely follows the southern edge of the oval, and the CG latitude of the southern edge of the irregularity zone can be followed as a function of local time. The aircraft contains a photometer and an auroral all-sky camera which were also operated but, because of partial cloud cover on this night, the all-sky camera data cannot be used. The 5577Å spectral line of the photometer operated very well through the cloud cover and responded to the presence of aurora in the zenith at 2140 LT (indicated in Figure 16 by an arrow). The onset of the F-layer irregularity zone overhead is then closely related to the presence of aurora in the zenith in the late evening sector. Bates (27) and Bates et al. (28), studying the correlation between radio and optical aurora in the night sector, noted close but not exact spatial coincidence between optical aurora and HF auroral backscatter. A study of the correlation between radio and optical aurora was not intended here, but it appears that the F-layer irregularity zone is closely related to the F region which Bates has identified as the source of HF backscatter.

The slant range plotter for October 28, 1970 is seen in Figure 17. The letter b indicates the presence of overhead blanketing E_{ss} which did not permit the detection of oblique incidence F-layer echoes. The presence of aurora in the zenith, noted by the arrow at 2000 LT, was again determined from the intensity of the 5577Å spectral line and it occurred about 1 3/4 hours earlier than on the previous night. Similarly, the irregularity zone, indicated by squares, was detected earlier than on the previous night. The daily sum of the geomagnetic activity indices, Kp, on Oct. 27 was $\Sigma Kp=9$ and on Oct. 28 was $\Sigma Kp=22+$. The difference in onset times of the irregularity zone on these two days can readily be explained by the difference in magnetic activity on the two days. If one puts the slant range data for these days onto auroral ovals of different Q value, then the reason for the difference in the onset times between the two days can be seen clearly. A Q=1 and a Q=3 oval were selected for the date of October 27 and 28 respectively, and they are seen in Figures 18 and 19. The data points are plotted on a CG local time and CG latitude grid. In general the data points fit the two different ovals quite well but, in Figure 19, there is a sudden departure of the data points from the southern edge of the oval at about 17 to 18 CG time. This appears to be a real effect because it was possible to follow an echo, similar to echo III in Figure 14, on each ionogram recorded during this period. If the reflecting surface underwent an latitudinal oscillation at this time, it could produce this effect. It appears then that the latitude of the southern edge of the F-layer irregularity zone can be monitored by plotting the slant ranges to certain oblique incidence echoes onto the slant range plotter.

3.4 CONCLUSIONS

A special analysis of vertical and oblique incidence F-layer echoes, seen on vertical incidence ionograms, was presented. Results from the analysis suggest that the latitude of the southern edge of the polar F-layer irregularity zone can be monitored, therefore, on the spot analysis of ground station ionograms from Goose Bay, Labrador, can probably lead to a real-time or near real-time monitoring of the poler F-layer irregularity zone for 6 to 8 hours of each day. Furthermore, the time when the main F-layer trough passes over Goose Bay can be specified on each day. The close coincidence which was shown to exist between the location of aurora and the F-layer irregularity zone suggests that the CG latitude of the southern edge of the auroral oval, in the afternoon and evening sectors, can similarly be monitored.

ACKNOWLEDGEMENTS

The authors wish to thank the following: D. Kimball, for the detailed evaluation of the all-sky photographs recorded on the flight of 14 December 1968; J.A. Whalen for comparison with his photometer data and helpful discussions, G.J. Gassmann, J. Buchau, R. Penndorf for valuable comments and discussions. The successful operation of all instruments was under the direction of R.W. Gowell, Major A.H. Sizoo coordinated the flight schedules, and the aircraft was operated by the aircrew members of Test Operations of the 3245th Air Base Group.

1. Hanson, G.H., Hagg, E.L., and Fowle, D., "The Interpretation of Ionospheric Records". Canadian Defense Research Telecommunications Estab. Rep. No. R-2, 1953.

2. Feldstein, Y.I. and Starkov, G.V., "Dynamics of Auroral Belt and Polar Geomagnetic Disturbances". Planet. Space Sci., 15, 209, 1967.

3. Hultqvist, B., "The Spherical Harmonic Development of the Geomagnetic Field, Epoch 1945, Transformed into Rectangular Geomagnetic Coordinate Systems". Arch. Geophys., 3, 53, 1958a.

4. Hultqvist, B., "The Geomagnetic Field Lines in Higher Approximation". Arch. Geophys., 3, 63, 1958b.

5. Hakura, Y., "Tables and Maps of Geomagnetic Coordinates Corrected by the Higher Order Spherical Harmonic Terms" Rep. Ionosphere Space Res. Japan, 19, 121, 1965.

6. Knecht, R.W., "Relationships between Aurora and Sporadic E Echoes at Barrow, Alaska". J. Geophys. Res., 61, 1, 59, 1956.

7. Buchau, J., Whalen, J.A., and Akasofu, S.-I., "Airborne Observation of the Midday Aurora". J. Atmos. Terr. Phys., 31, 1021, 1969.

8. Whalen, J.A., Buchau, J., and Wagner, R.A., "Airborne Ionospheric and Optical Measurements of Noontime Aurora". J. Atmos. Terr. Phys., 33, 661, 1971.

9. Hunsucker, R.A. and Owren, L., "Auroral Sporadic E Ionization". J. Res. Nat. Bureau of Standards, 66D, 581, 1962.

10. Harang, L., "The Aurorae". John Wiley and Sons, Inc., New York, 1951.

11. Pittenger, E.W. and Gassmann, G.J., "High Latitude Sporadic E". AFCRL Environmental Research Paper, No. 347, 1971.

12. Penndorf, R., "High-Latitude Propagation Study". RADC-TR-70-240, Vol. 1, Final Technical Report, 1971.

13. King, G.A.M., "The Aurora and the Night E layer". J. Atmos. Terr. Phys., 27, 426, 1965.

14. Bullen, J.M., "Enhanced Activity in the Ionosphere E Region at Cape Hallet and Campbell Island". J. Atmos. Terr. Phys., 28, 879, 1966.

15. King, G.A.M., "The Night E Layer", in "Ionospheric Sporadic E". E.K. Smith and S. Matsushita, Ed., Pergamon Press, New York, 219, 1962.

16. IGY Instruction Manual, The Ionosphere, Annals of the International Geophysical Year, Vol. III, Pergamon Press, 1957.

17. Whalen, J.A., Private Communication, AFCRL.

18. Muldrew, D.B., "F-Layer Ionization Troughs Deduced from Alouette Data". J. Geophys. Res., 70, 11, 2635, 1965.

19. Petrie, L.E., "Preliminary Results on Mid and High Latitude Spread F", in "Spread F and Its Effect on Radio Wave Propagation and Communication". AGARDograph 95, edited by Philip Newman, Technivision Press, 67, 1966.

20. Akasofu, S.-I., "Polar and Magnetospheric Substorms". D. Reidel Publishing Company, Dordrecht, 1968.

21. Thomas, J.O. and Andrews, M.K., "The Trans-polar Exospheric Plasma, 3: A Unified Picture". Planet. Space Sci., 17, 439, 1969.

22. Pike, C.P., "A Latitudinal Survey of the Daytime Polar F Layer". J. Geophys. Res., to appear 1971.

23. Stanley, G.M., "Ground-Based Studies of the F Region in the Vicinity of the Mid-Latitude Trough". J. Geophys. Res., 71, 21, 5067, 1966.

24. Bowman, G.G., "Ionization Troughs Below the F2-Layer Maximum". Planet. Space Sci., 17, 777, 1969.

25. Bates, H.F., "The Aspect Sensitivity of Spread-F Irregularities". J. Atmos. Terr. Phys., 33, 111, 1971.

26. Thomas, J.O. and Rycroft, M.J., "The Exospheric Plasma During the International Years of the Quiet Sun". Planet. Space Sci., 18, 41, 1970.

27. Bates, H.F., Belon, A.E., Romick, G.J., and Stringer, W.J., "On the Correlation of Optical and Radio Auroras". J. Atmos. Terr. Phys., 28, 439, 1966.

28. Bates, H.F., Sharp, R.D., Belon, A.E., and Boyd, J.S., "Spatial Relationships Between HF Radar Aurora, Optical Aurora and Electron Precipitation". Planet. Space Sci., 17, 83, 1969.

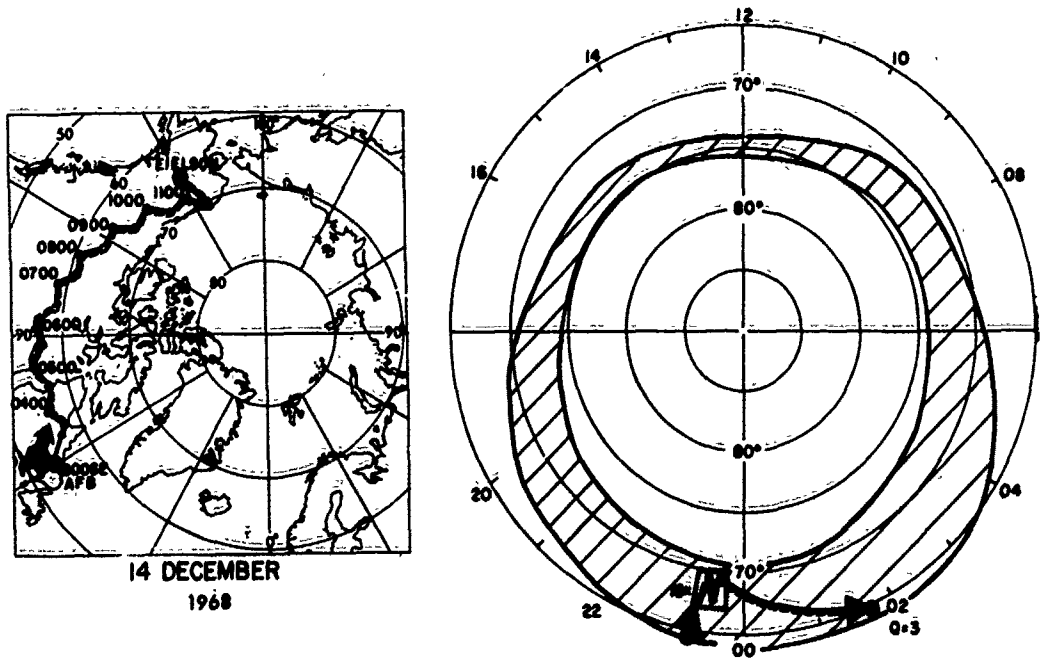

Figure 1. Flight track of the flight of 14 December 1968 in geographic (left) and CG coordinates (right). The Q=3 oval is indicated by heavy solid lines.

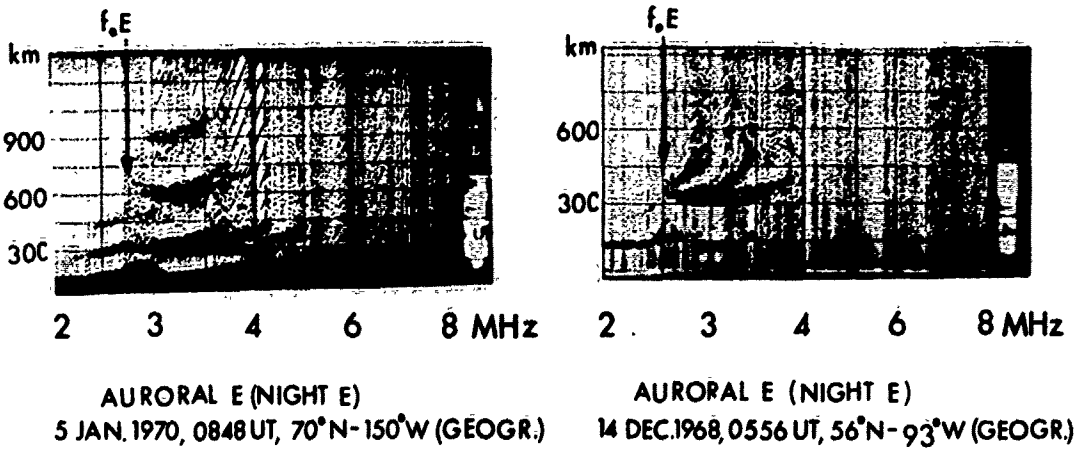

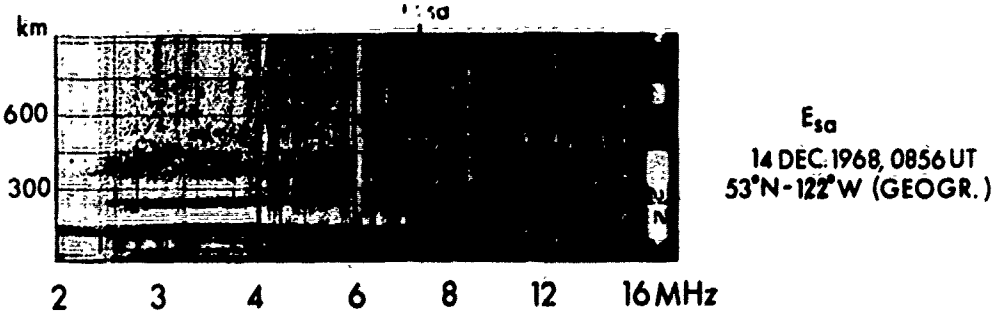

Figure 2. Examples of ionograms which show night E (auroral E) and E_{sa} echoes.

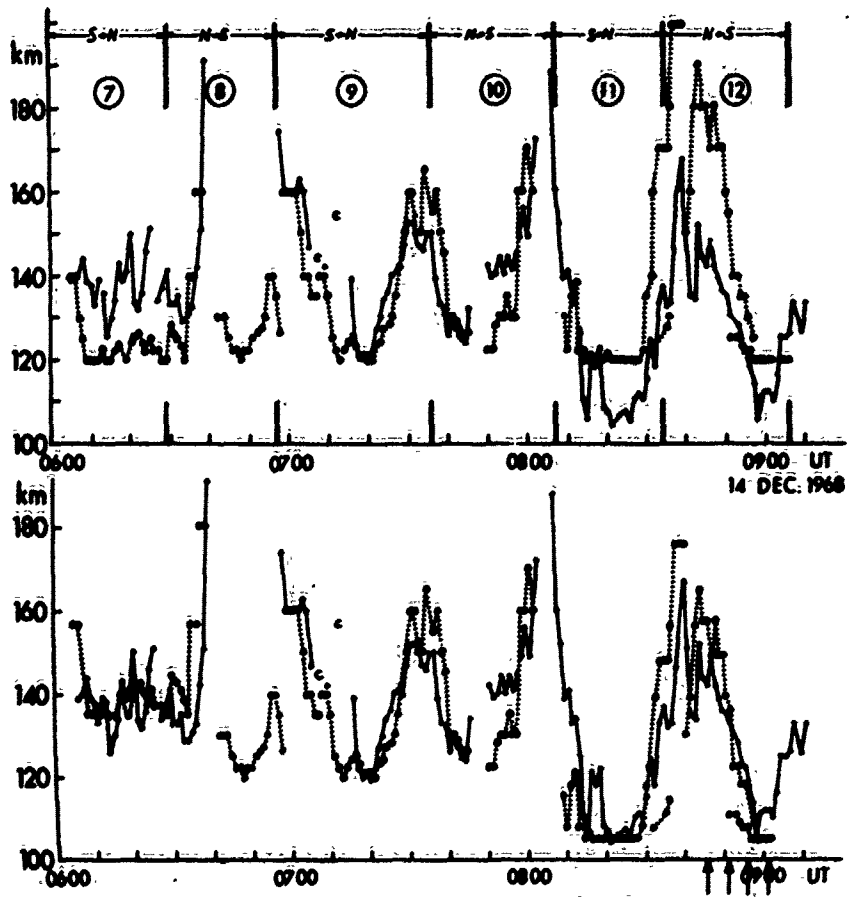

Figure 3. Virtual heights of E_{ss} versus UT, open circles; and slant ranges to the aurora versus UT, full circles, connected by dotted lines. The encircled numbers are the numbers in the sequence of 18 latitudinal scans. The vertical double lines indicate the aircraft turns at the northern or southern end of the scans. Upper part: slant ranges to the aurora, when actual height of aurora is assumed to be 120 km above ground; lower part: slant ranges to the aurora when actual height of aurora is assumed to be identical to the virtual height of E_{ss}, measured when aurora is overhead. The arrows on the abscissa mark the times when the ionograms and all-sky photographs, shown in Figure 5, were recorded.

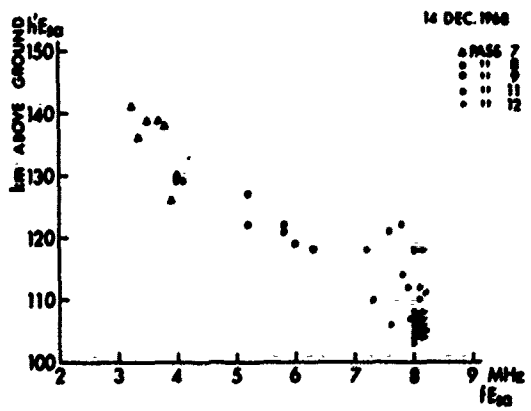

Figure 4. Virtual height of E_{ss} echo versus top frequency of E_{ss} for 14 December 1968. The values were recorded when aurora was overhead. The arrows at some of the 8 MHz values indicate that the top frequencies were higher than the high frequency limit of the sweep.

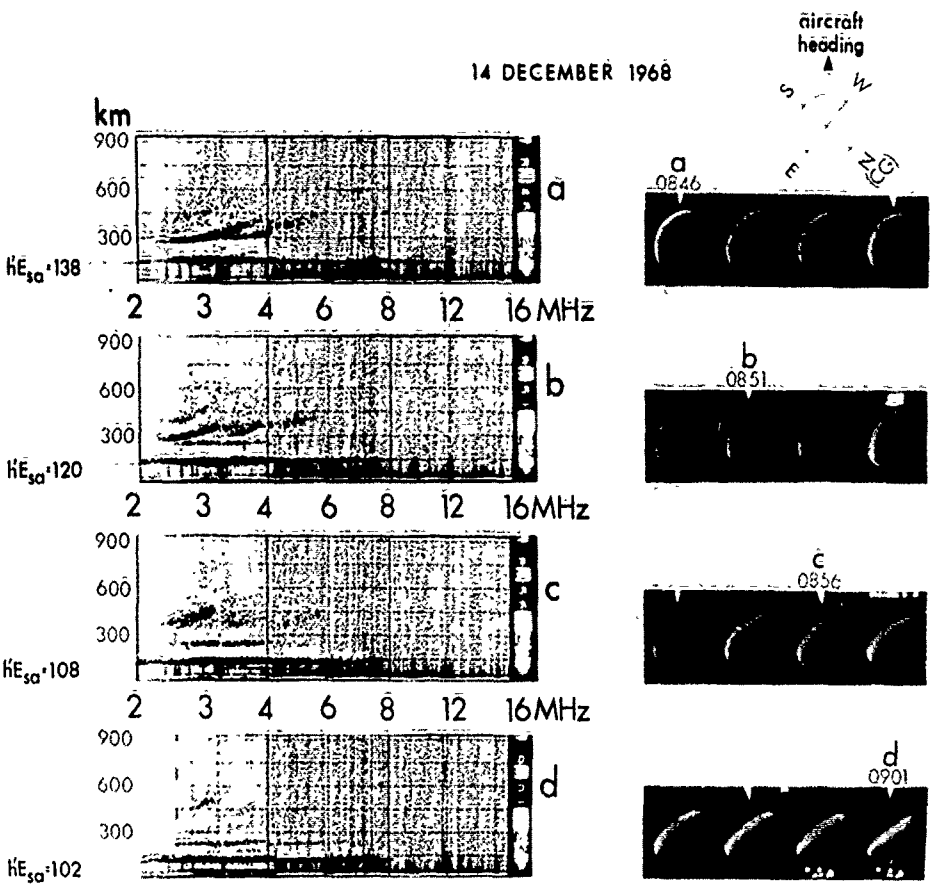

Figure 5. Ionograms and all-sky photographs simultaneously recorded on 14 December 1968, pass 12.

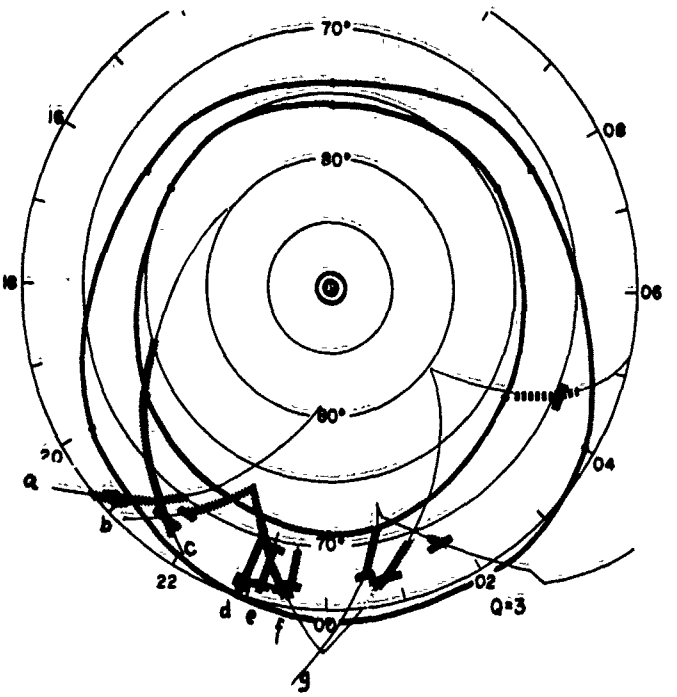

Figure 6. Flight tracks of flights through the night sector of the auroral oval; thick dotted lines mark the latitudes where night E (auroral E) was observed; black bars indicate the location of maximum f_0E for each latitudinal scan: a) 10/11 October 1969, b) 21 April 1969, c) 12 and 14 Dec 1969, d) 24 November 1970, e) 1/2 February 1971, f) 14 December 1968, and g) 5/6 February 1968.

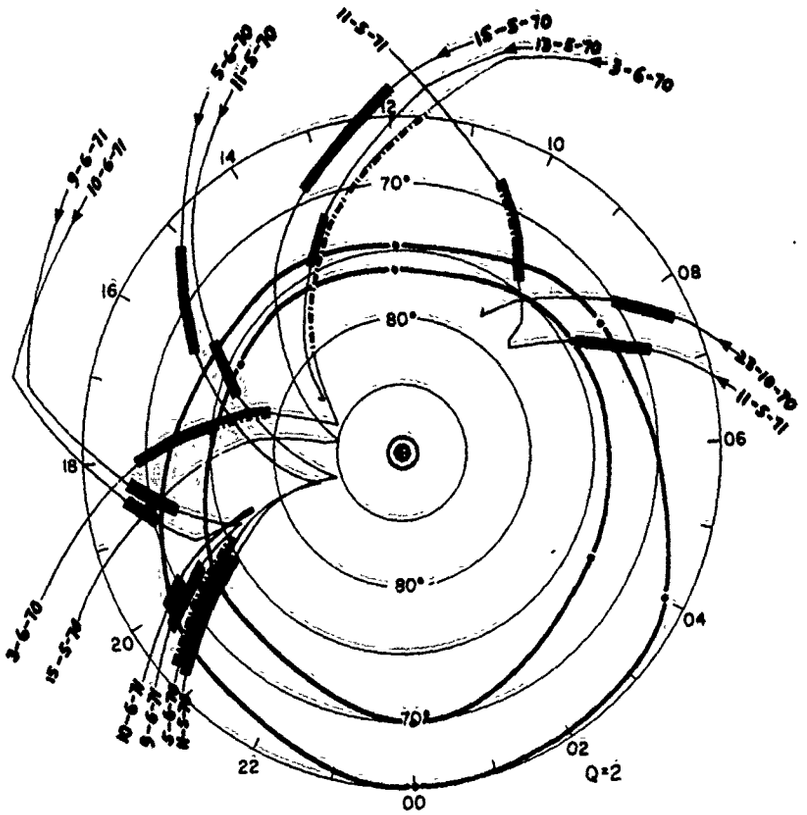

Figure 7. Flight tracks of cross-sections through the oval in daylight conditions. Latitudes where enhanced f_0E was observed are marked by thick black lines; dotted sections are less certain.

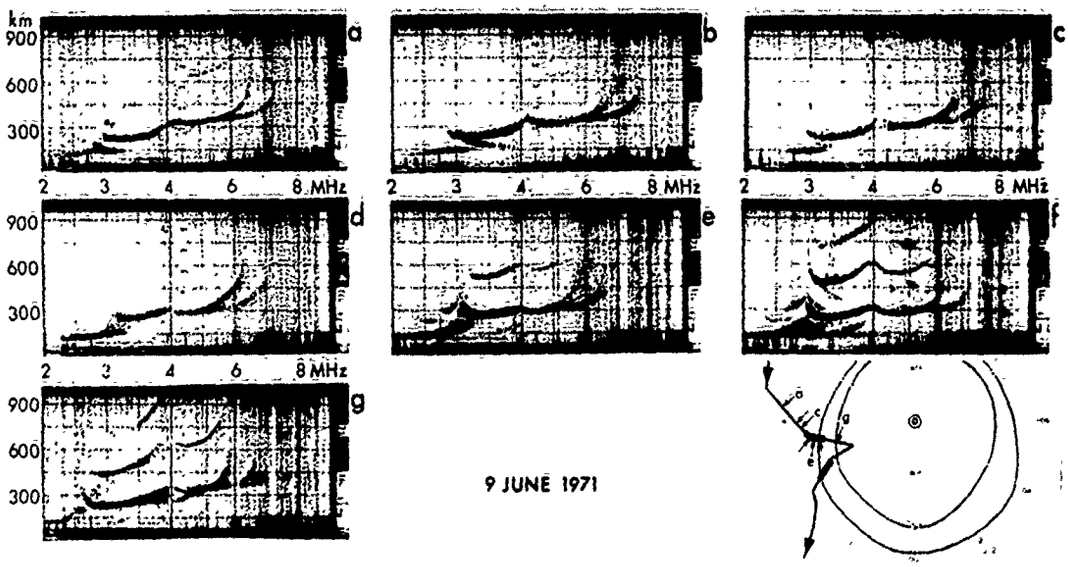

Figure 8. Ionograms recorded on a flight traversing a region where enhanced f_0E was observed on 9 June 1971. On the flight track, plotted in CG coordinates, heavy lines indicate the latitudes of enhanced f_0E. The arrows mark the locations where ionograms a. through g. were recorded.

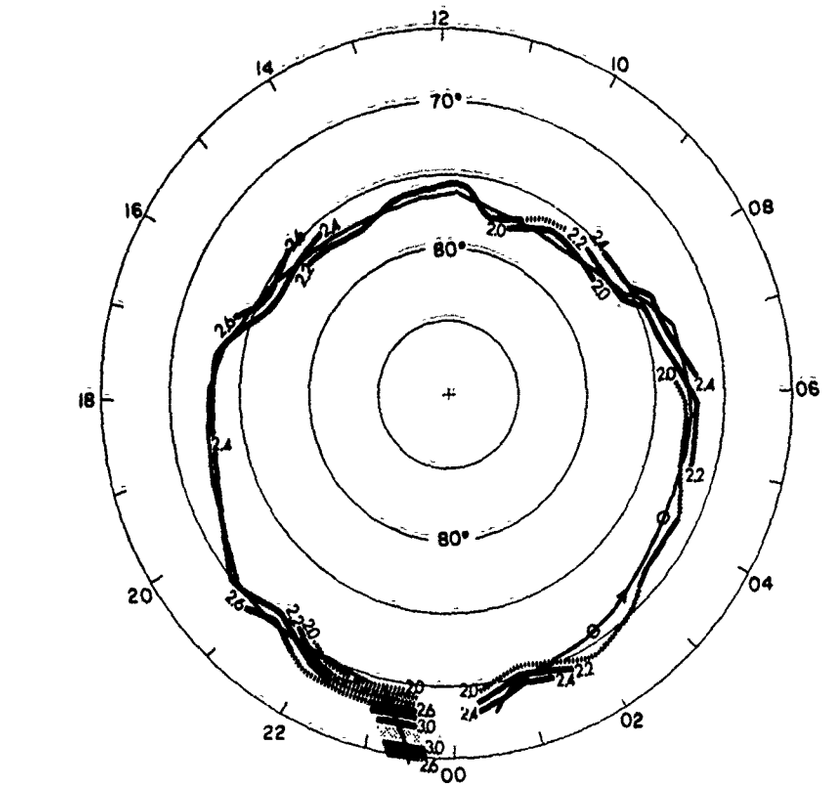

Figure 9. Contours of f_0E for the flight of 5 January, 1970.

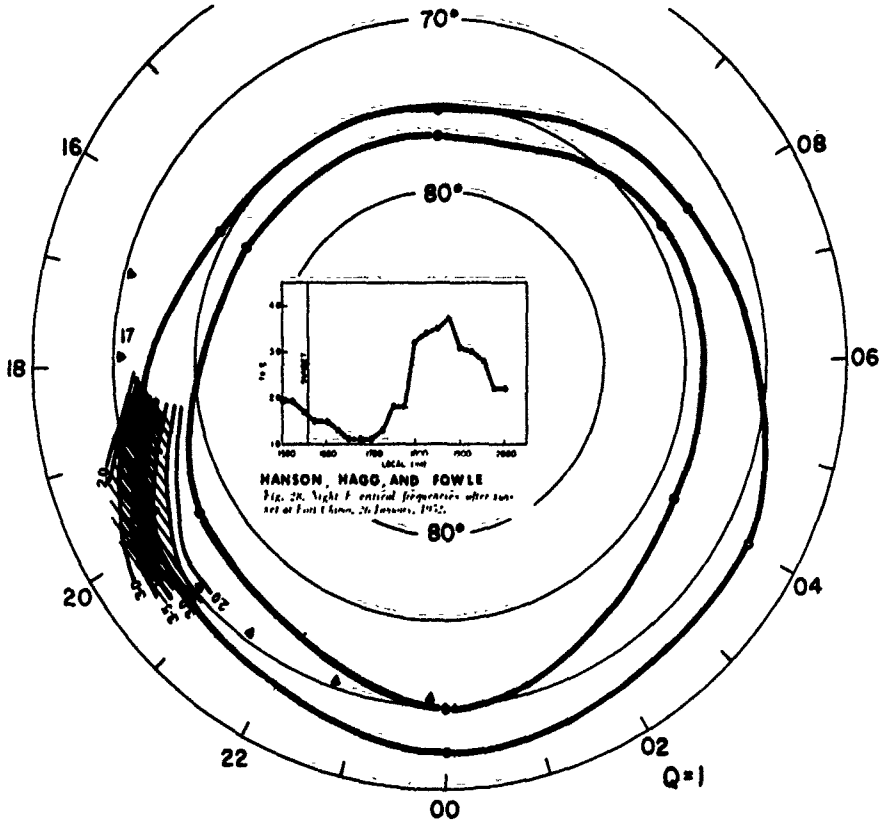

Figure 10. Time variation of f_0E as experienced by a ground station moving, relative to the oval, through a belt of E ionization.

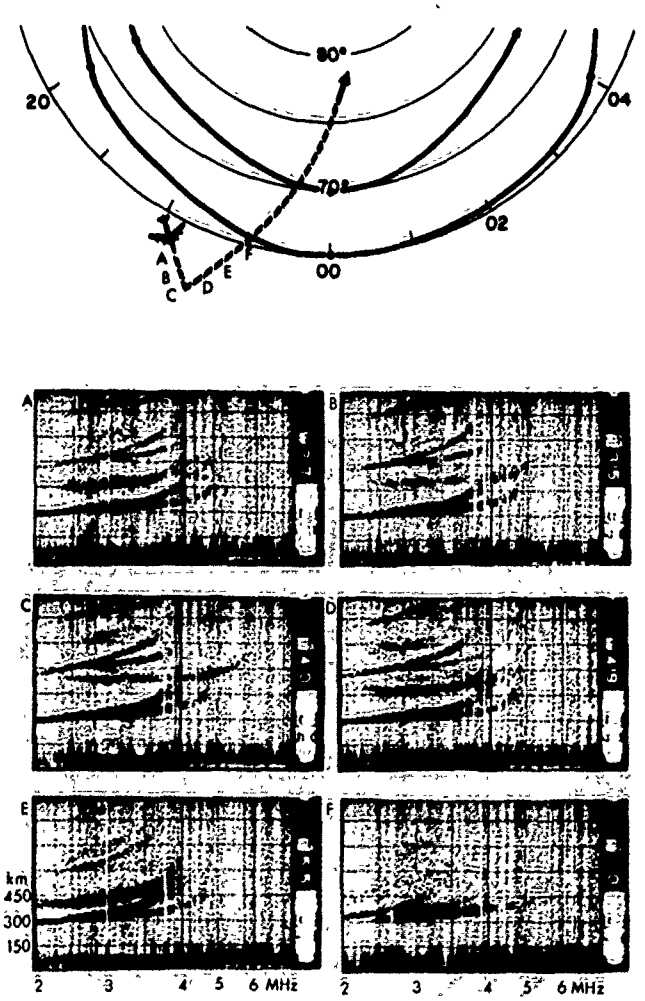

Figure 11. Aircraft flight route on August 22, 1970 is drawn on a CG latitude and CG local time grid. The night sector of the Q=2 auroral oval is indicated by heavy solid lines. A sequence of airborne ionograms, recorded at the positions marked by letters next to the flight route, is shown.

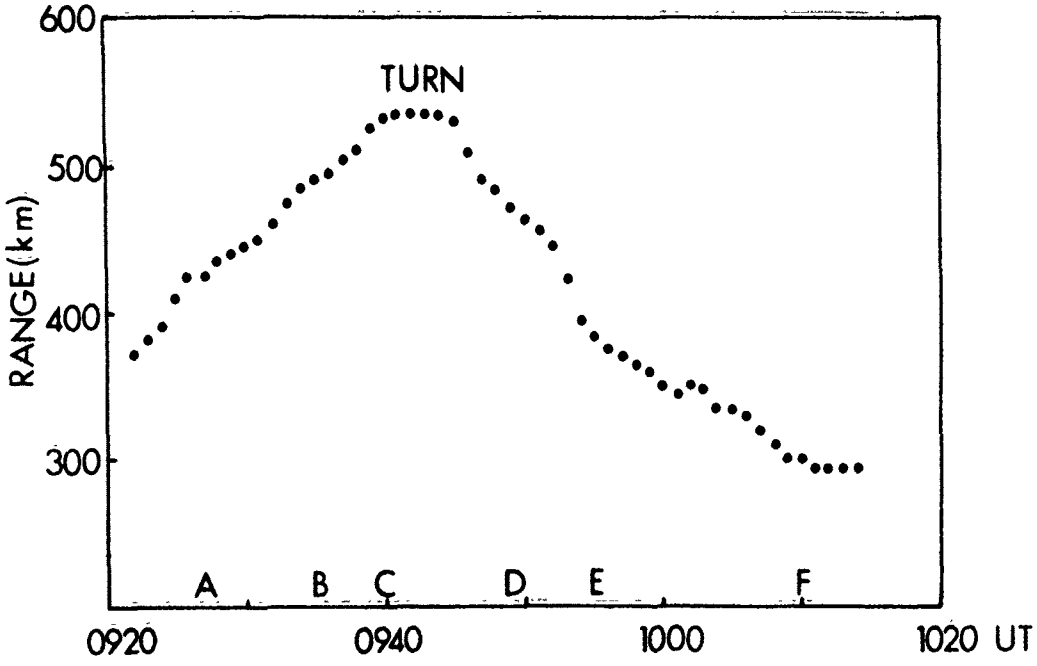

Figure 12. The slant range to the extra echo seen in the airborne ionogram sequence is plotted versus universal time. The letters refer to the aircraft's position.

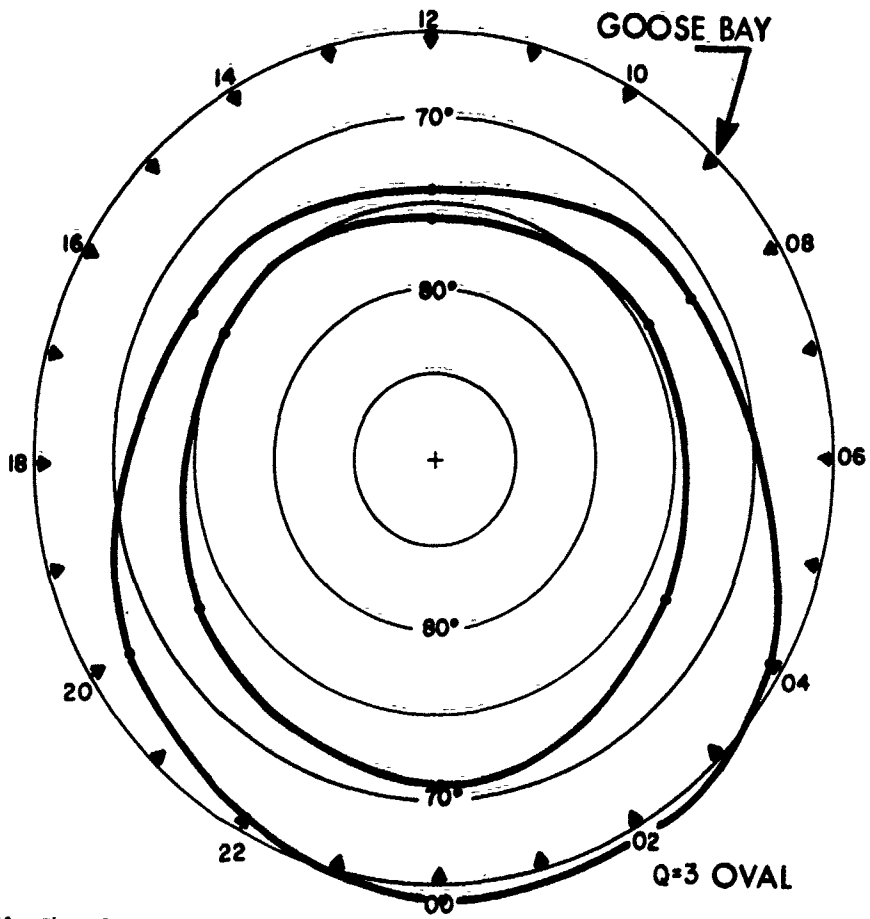

Figure 13. The Q=3 auroral oval is plotted on a grid of CG latitude and CG local time, and the location of Goose Bay is indicated by triangles.

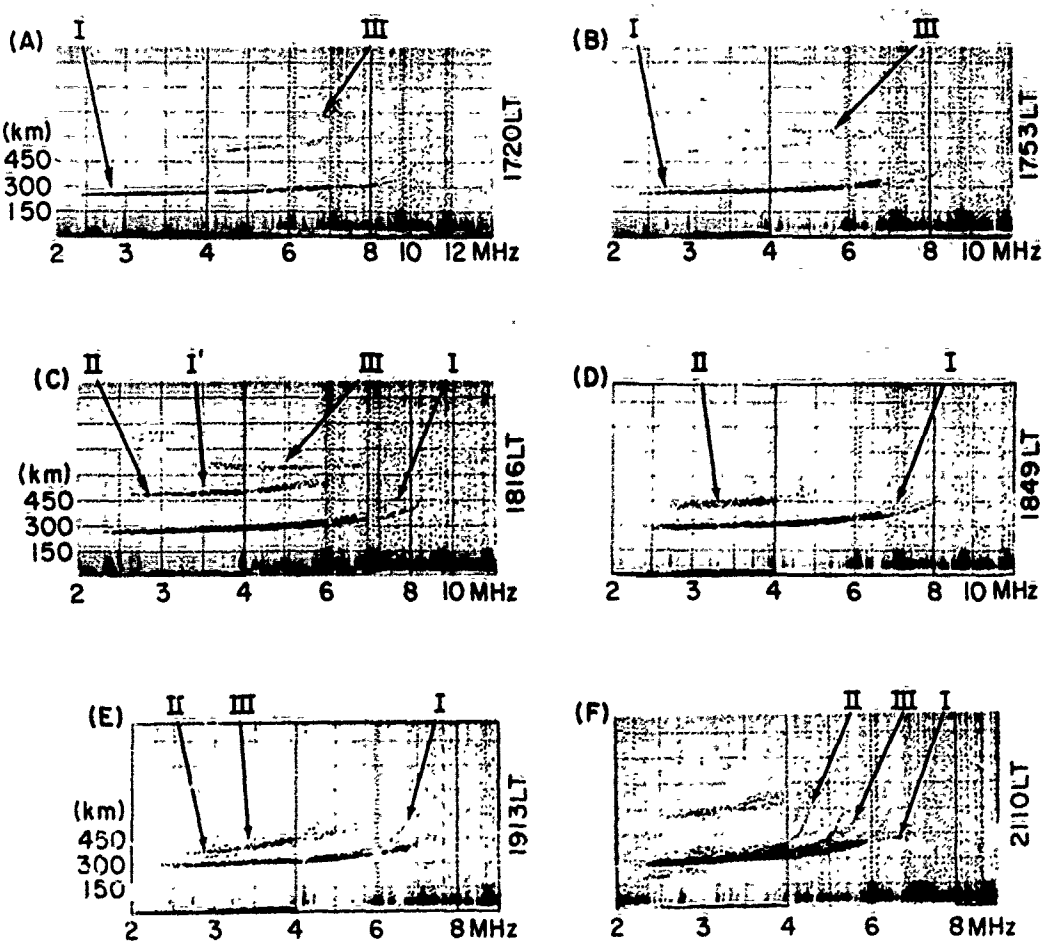

Figure 14. Goose Bay ionograms recorded on October 27, 1970.

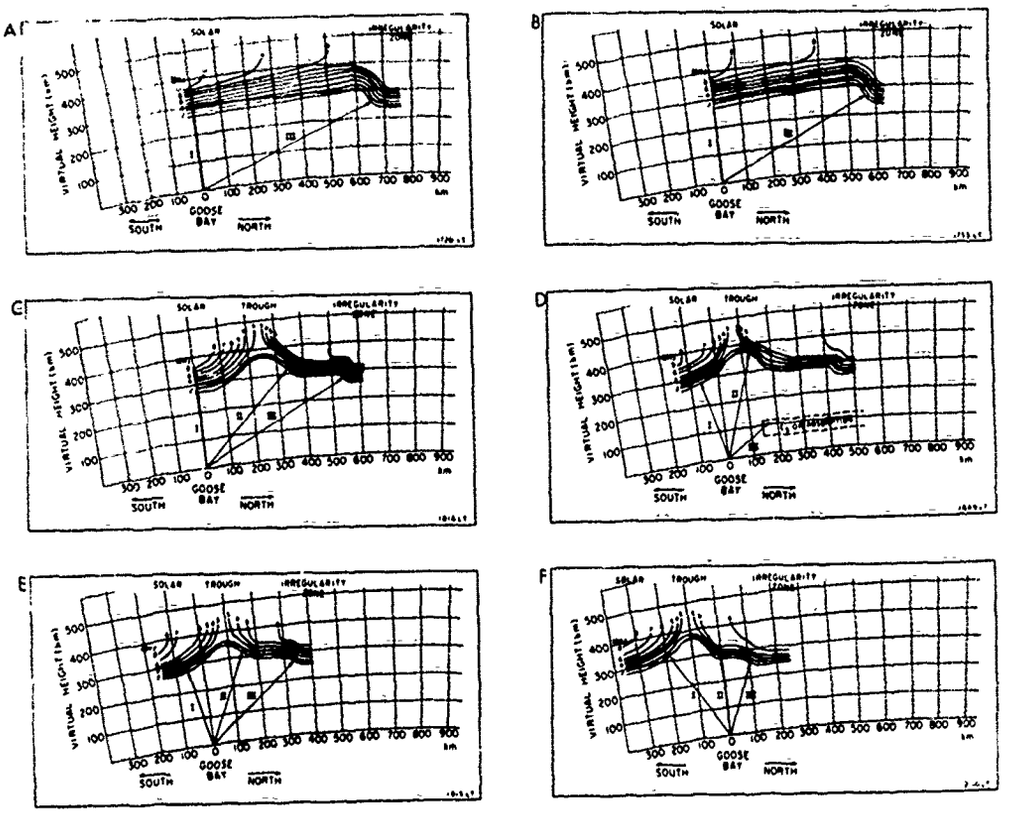

Figure 15. Schematic drawings of plasma frequency contours over Goose Bay are shown.

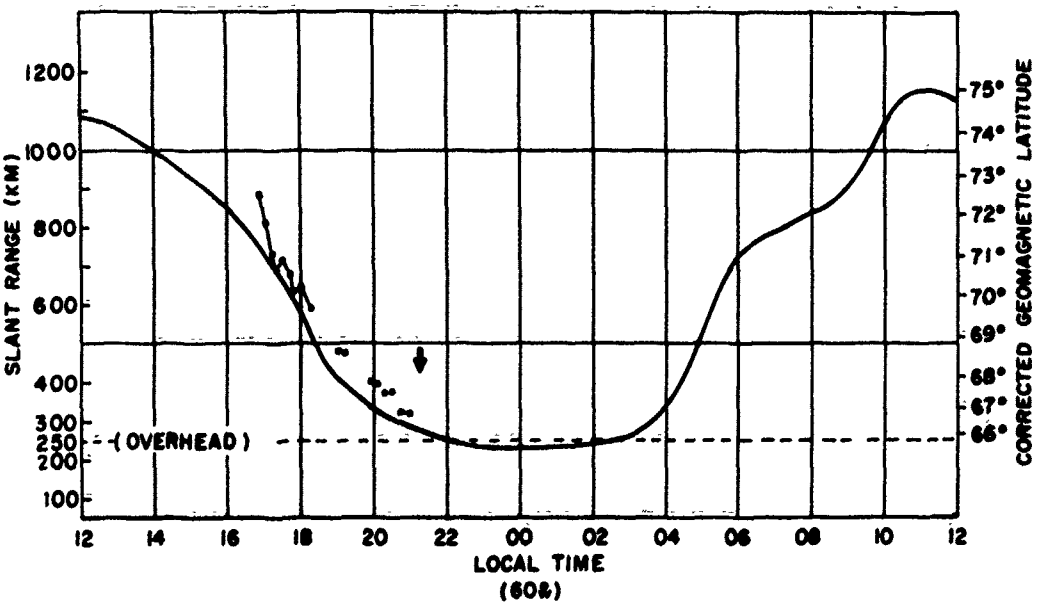

Figure 16. The slant range to the southern edge of the auroral oval from Goose Bay is plotted as a heavy solid line versus 60°W local time. The slant range to the F-layer irregularity zone from Goose Bay on October 27, 1970 is indicated by squares. An arrow indicates the onset of aurora in the zenith at Goose Bay.

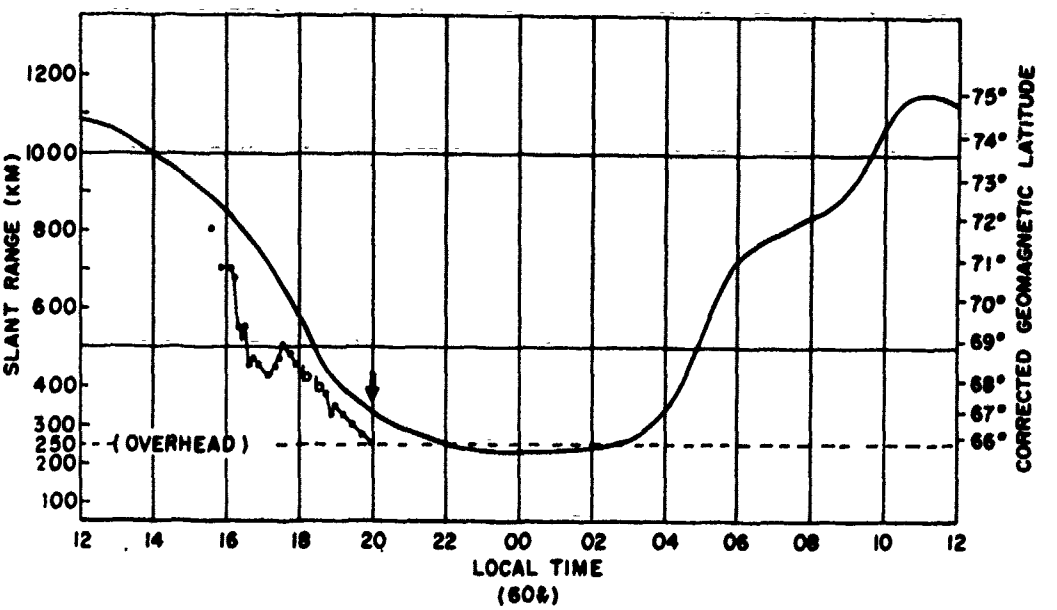

Figure 17. The slant range to the southern edge of the auroral oval from Goose Bay is plotted as a heavy solid line versus 60°W local time. The slant range to the F-layer irregularity zone from Goose Bay on October 28, 1970 is indicated by squares. An arrow indicates the onset of aurora in the zenith at Goose Bay.

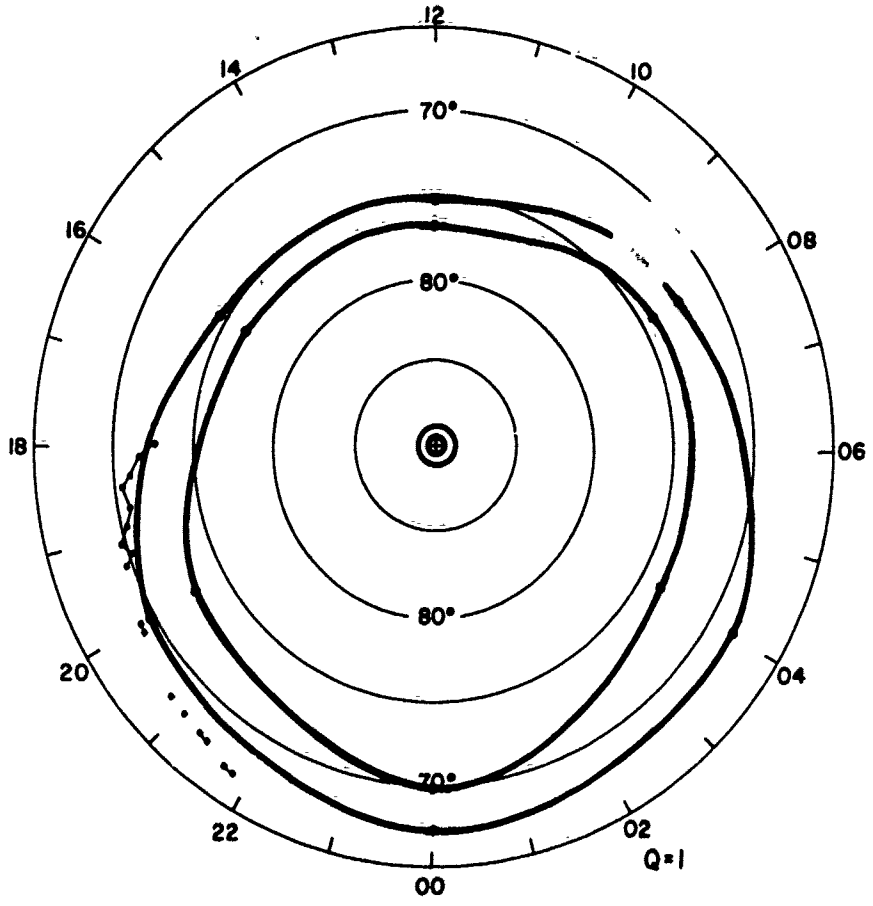

Figure 18. The latitude of the southern edge of the F-layer irregularity zone on October 27, 1970, indicated by squares, is plotted on a CG latitude and CG local time grid. The Q=1 oval is indicated by heavy solid lines.

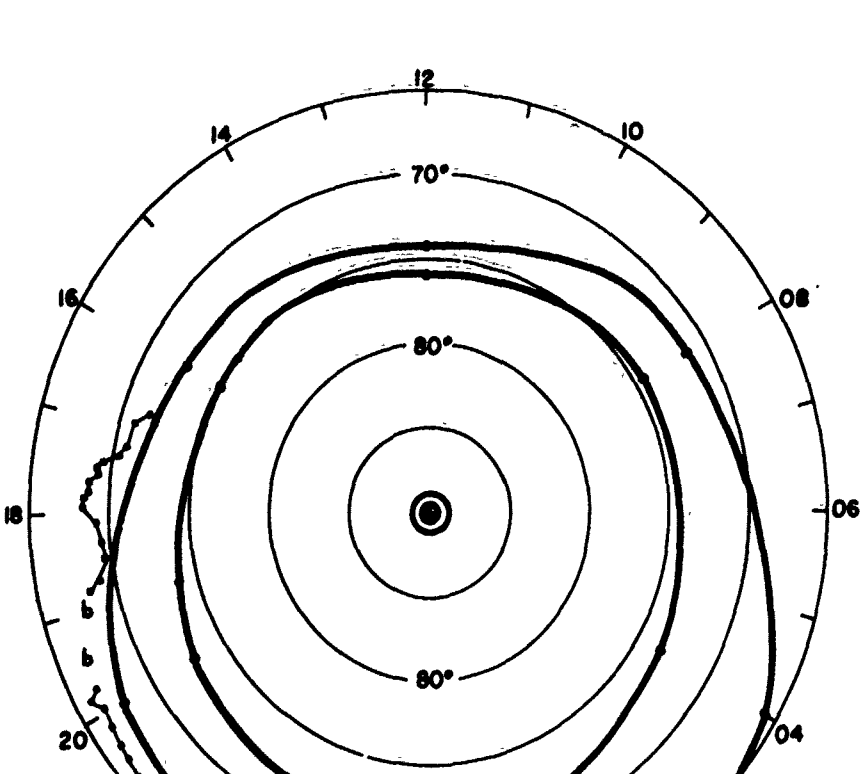

Figure 19. The latitude of the southern edge of the F-layer irregularity zone on October 28, 1970, indicated by squares, is plotted on a CG latitude and CG local time grid. The Q=3 oval is indicated by heavy solid lines. The letter b indicates the presence of blanketing E_{ss}.